

Pseudo-Bag Mixup Augmentation for Multiple Instance Learning-Based Whole Slide Image Classification

Pei Liu, Luping Ji *Member, IEEE*, Xinyu Zhang, and Feng Ye

Abstract—Given the special situation of modeling gigapixel images, multiple instance learning (MIL) has become one of the most important frameworks for Whole Slide Image (WSI) classification. In current practice, most MIL networks often face two unavoidable problems in training: i) insufficient WSI data, and ii) the sample memorization inclination inherent in neural networks. These problems may hinder MIL models from adequate and efficient training, suppressing the continuous performance promotion of classification models on WSIs. Inspired by the basic idea of Mixup, this paper proposes a new Pseudo-bag Mixup (PseMix) data augmentation scheme to improve the training of MIL models. This scheme generalizes the Mixup strategy for general images to special WSIs via pseudo-bags so as to be applied in MIL-based WSI classification. Cooperated by pseudo-bags, our PseMix fulfills the critical size alignment and semantic alignment in Mixup strategy. Moreover, it is designed as an efficient and decoupled method, neither involving time-consuming operations nor relying on MIL model predictions. Comparative experiments and ablation studies are specially designed to evaluate the effectiveness and advantages of our PseMix. Experimental results show that PseMix could often assist state-of-the-art MIL networks to refresh the classification performance on WSIs. Besides, it could also boost the generalization ability of MIL models, and promote their robustness to patch occlusion and noisy labels. Our source code is available at <https://github.com/liupeil101/PseMix>.

Index Terms—Computational Pathology, Data Augmentation, Pseudo-Bag Mixup, Multiple Instance Learning, Whole Slide Image Classification.

I. INTRODUCTION

Histological Whole-Slide Image (WSI) serves as the gold standard of pathology diagnosis and plays a vital role in cancer assessment and treatment [1]–[3]. Owing to the advances in deep learning, many clinical tasks with WSIs, such as lymph node metastasis detection, cancer subtyping, and cancer prognosis, have been made automatic and precise by specialized models [4]–[15]. These models show exciting progress towards overcoming the long-standing drawbacks of manual inspection [16], [17]. Across them, a weakly-supervised learning framework called multiple instance learning (MIL) is widely used. It treats a gigapixel WSI (e.g., $40,000 \times 40,000$ pixels) as a bag of multiple instances, and learns a global image representation via instance embedding and aggregation [18].

Pei Liu, Luping Ji, and Xinyu Zhang are with the School of Computer Science and Engineering, University of Electronic Science and Technology of China, Chengdu 611731, China.

Feng Ye is with the Institute of Clinical Pathology, West China Hospital, Sichuan University, Guo Xue Xiang, Chengdu 610041, China.

* Corresponding author: Luping Ji (jiluping@uestc.edu.cn).

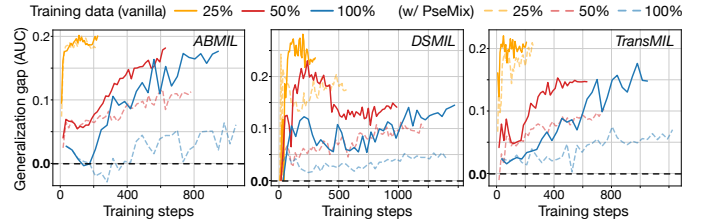


Fig. 1. Generalization gap of MIL models during training. It is measured by the model performance gap between training and test sets, to assess the generalization ability of models, following [20], [21]. Three state-of-the-art MIL models are trained on BRCA WSI samples. Vanilla models often show growing gaps. The models trained with our PseMix could alleviate these without introducing extra complicated techniques.

This framework enables neural network (NN) models to handle gigapixel images and no longer rely on fine-grained instance-level labels. For those reasons, MIL has become a prevalent paradigm for WSI classification, achieving considerable success in computational pathology (CPATH) [19].

Nonetheless, our empirical study, as presented in Figure 1, reveals that some state-of-the-art MIL models [8], [9], [18] often perform poorly in generalization, even worse in probable small data scenarios. The literature on learning theory and NNs [22]–[24] points out that such kind of problem is the consequence of *data memorization*, fundamentally caused by the nature of NNs and existing even in the presence of strong regularization. Due to internal data memorization characteristics, MIL networks could merely memorize, rather than efficiently learn or generalize from, given training samples, thus limiting the model performance on unseen test data and increasing generalization gaps. Besides, as an external cause, insufficient samples may hinder models from inadequate training, further degrading generalization performance. In contrast to a multitude of studies on classical image classification for alleviating the data memorization problem in models [20], [25], the current works on WSI classification rarely formally investigate this problem in MIL. Thereby, most modern MIL models still carry the risk of inadequate and inefficient training, suppressing their continuous performance promotion.

Mixup [26], as a special data augmentation method, shows great promise in mitigating the inherent data memorization in NNs. Unlike most augmentation methods that only manipulate single input, Mixup operates on two inputs and generates the interpolation samples between them ($\tilde{x} = \lambda x_i + (1 - \lambda)x_j$, $\tilde{y} = \lambda y_i + (1 - \lambda)y_j$). These interpolation-based samples are also interpreted as neighbor or vicinity samples, leveraged

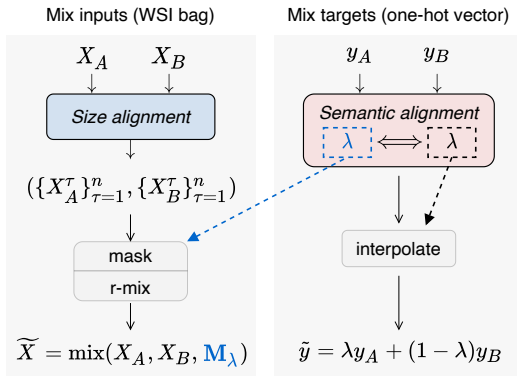


Fig. 2. A conceptual framework of PseMix for MIL-based WSI classification. X_A^τ and X_B^τ denote pseudo-bags. M_λ is a binary mask. R-mix means random mixing. PseMix generalizes Mixup and fulfills its critical size alignment and semantic alignment via pseudo-bags.

as augmented data for training. In this particular way, NNs are never limited to memorizing finite training samples from the original distribution; instead, they are encouraged to learn from the vicinity distribution of training samples and obtain a decision boundary with better generalization [26]. Such a simple yet efficient method has been developed and witnessed remarkable success in its application to heterogeneous data, *e.g.*, natural image [27]–[29], graph [30], 3D point cloud, [31], visual-language [32], etc. Further adoption of Mixup for histological WSIs is strongly anticipated. However, the characteristic of WSIs poses several challenges to it. Unlike other data sources, i) histological WSIs are usually cast as bags for weakly-supervised MIL; ii) WSI bags are often irregular and not well-aligned in Euclidean space for interpolation (*i.e.*, $\tilde{x} = \lambda x_i + (1 - \lambda)x_j$); and iii) a single bag may contain tens of thousands of instances, each with a high-dimensional feature vector [7]. These characteristics suggest that a practical and suitable Mixup method for WSIs should be compatible with MIL, capable of mixing alignment, and efficient.

For the purposes above, this paper proposes a new Pseudo-bag Mixup (PseMix) data augmentation scheme, as illustrated in Figure 2. We address the challenges aforementioned from the following three aspects. (1) *MIL compatibility*: our scheme takes WSI bags as input and outputs the mixed bags that still could be processed by MIL. (2) *Mixing alignment*: we divide each bag into n pseudo-bags for size alignment in bag mixing, and share the λ between bag mixing and target mixing for semantic alignment. (3) *Efficiency*: our pseudo-bag division is designed as an algorithm with linear time and space complexity, and PseMix is decoupled from the stage of MIL so as to be plugin-and-play. In addition, our PseMix further introduces a random mixing mechanism (*i.e.*, r-mix in Figure 2) for more data diversity and efficient learning on vicinity samples. Comparative experiments confirm that our PseMix could serve as an effective Mixup data augmentation method. Apart from the improvements across three different classification tasks, the models trained with our PseMix could often surpass vanilla models by a large margin in various generalization and robustness tests.

The main contributions of this paper are as follows. (1)

This paper proposes a new Pseudo-bag Mixup (PseMix) data augmentation scheme for MIL-based WSI classification, to help MIL models improve performance and obtain better generalization, as well as robustness. It is an efficient and plugin-and-play one, neither involving time-consuming operations nor relying on the prediction of MIL models. (2) This paper generalizes the Mixup strategy for common images to special WSIs by the critical size and semantic alignment on pseudo-bags. Furthermore, it introduces a random mixing mechanism into standard Mixup for more data diversity and efficient learning on augmented mixing samples. (3) Comparative experiments, ablation study, and various scenarios, *e.g.*, usual WSI classification, generalization test, the robustness test on patch occlusion and noisy labels, etc, are specially designed to demonstrate the broad advantages of PseMix.

II. RELATED WORK

A. Multiple instance learning for WSI classification

Multiple instance learning (MIL) [18] nowadays has been increasingly used in computational pathology for weakly-supervised WSI classification [4]–[15]. Its regular procedure [19] on gigapixel WSIs could be decomposed into two main stages: i) WSI preprocessing, each digital slide is transformed into a bag of instances through patching and patch feature extracting; and ii) weakly-supervised MIL, a bag is compressed into a global vector for slide-level prediction by a MIL network [18]. The first stage is computationally intensive because of the transformation from gigapixel images to massive feature vectors. Thus, this stage is usually fixed for saving computational costs, not involved in training [35], [36].

B. Mixup data augmentation

The basic idea of Mixup [26] could be formulated as follows:

$$\tilde{x} = \lambda x_i + (1 - \lambda)x_j, \quad \tilde{y} = \lambda y_i + (1 - \lambda)y_j, \quad (1)$$

where the two samples (x_i, y_i) and (x_j, y_j) are drawn from training data, and $\lambda \in [0, 1]$ follows a Beta distribution with a parameter $\alpha \in [0, +\infty]$. Despite its simplicity, Mixup has been proven, empirically and theoretically, to be an effective and practical data augmentation strategy across many different fields for improving the generalization and robustness of deep learning models [21], [27]–[32], [37].

From an alignment perspective, we could observe the two critical factors in the Mixup formulation given by Equation 1. (1) Size alignment, *i.e.*, x_i and x_j must be aligned in Euclidean space before mixing. (2) Semantic alignment, *i.e.*, the mixed input \tilde{x} is derived from x_i and x_j , and its content is controlled by λ , so its corresponding label \tilde{y} should be associated with y_i and y_j , and its value should be determined by the same λ . Based on this perspective, the state-of-the-art Mixup variants for different data sources could be summarized in a unified form, as exhibited in the top half of Table I.

Apart from interpolation, masking is also one of the most important ways for input mixing implementation. In the domain of image classification, it is reported [29] that masking-based Mixup variants often perform better than interpolation-based ones because interpolation operation treats background

TABLE I
RELATED DATA AUGMENTATION METHODS. THE MIX MANNER, R-MIX, MEANS RANDOM MIXING.

| Method | Data type | Input | | | Target | |
|----------------------------------|---------------|-------|----------------------|--------------|--------|-----------------------------|
| | | Mix | Size alignment | Mix manner | Mix | Semantic alignment |
| Mixup (2018) [26] | data-agnostic | ✓ | aligned by default | interpolate | ✓ | input interpolation scale |
| TransMix (2022) [29] | natural image | ✓ | scaling or cropping | mask & mix | ✓ | target attention weights |
| \mathcal{G} -Mixup (2022) [30] | graph | ✓ | graphon estimation | interpolate | ✓ | graphon interpolation scale |
| PointPatchMix (2023) [31] | point cloud | ✓ | point patch | mask & mix | ✓ | patch attention scores |
| Pseudo-bag (2021) [6] | WSI | ✗ | — | — | ✗ | — |
| ReMix (2022) [33] | WSI | ✓ | bag prototype | mask & mix | ✗ | — |
| RankMix (2023) [34] | WSI | ✓ | ranking and dropping | interpolate | ✓ | bag interpolation scale |
| PseMix (ours) | WSI | ✓ | pseudo-bag | mask & r-mix | ✓ | pseudo-bag mixing ratio |

and foreground equally and often yield meaningless samples. However, these leading Mixup methods could not be directly or efficiently applied to gigapixel WSIs, as WSIs are yet another kind of heterogeneous data, usually cast as irregular bags containing many high-dimensional instances [7], [19].

C. Data augmentation for multiple instance learning

Traditional image-level data augmentation methods [38], such as flipping, rotation, blurring, etc, have been adopted in WSI analysis [39], [40]. They are utilized in the stage of WSI preprocessing to generate different instance features for the same patch image, aiming to increase the diversity of instance-level features. However, this manner is computationally expensive for gigapixel images, because there are usually tens of thousands of patch images and each one needs multiple feature extraction even for a single WSI [35], [36].

The other methods, specially designed for MIL-based WSI classification, could be roughly divided into two categories: i) embedding-level data augmentation and ii) instance-level or bag-level data augmentation. The former focuses on augmenting instance embeddings with bag prototypes [33], generative adversarial networks [35], or diffusion models [41]. The latter mainly generates new subsets from bags via hierarchical [6], [42] or random sampling [11]. However, these methods have not yet explored the basic idea of Mixup.

As shown in the bottom half of Table I, although ReMix [33] proposes to mix two bag inputs, it restricts the mix within the same class, not falling into the range of Mixup [26]. Most recently, RankMix [34], as a Mixup variant, studies the basic idea of Mixup for WSI classification. It strictly follows the original interpolation way for bag mixing. However, it heavily relies on MIL networks to obtain instance attention scores for importance ranking and instance alignment. Unfortunately, there are often potential biases between attention scores and instance importance, as highlighted in [43]. Accordingly, there is still room for exploring Mixup on WSI data.

III. METHOD

In this section, we elaborate on how Mixup can be generalized to WSI classification via pseudo-bags, and introduce our random mixing mechanism. In the design of PseMix, we consider algorithm efficiency to make it practical and efficient to apply. Moreover, our PseMix is decoupled from the stage of MIL, so it is plugin-and-play for MIL models.

A. Preliminary

1) *Notation and convention*: As shown in Figure 3(a), a single digital slide is sliced into image patches, and then is processed into high-dimensional vectors by a feature extractor [7]. These feature vectors are taken as a bag of multiple instances. Given N slides, we denote their processed data by

$$\mathcal{D} = \{(X_i \in \mathbb{R}^{m_i \times d}, y_i)\}_{i=1}^N, \quad (2)$$

where X_i is the i -th bag, m_i is instance number, d means the dimension of each feature vector, and y_i is a slide-level label. Let $x_{i,j} \in \mathbb{R}^d$ denote the j -th instance of the i -th bag, hence $X_i = \{x_{i,j}\}_{j=1}^{m_i}$. Let $\{X_i^\tau\}_{\tau=1}^n$ represent the n pseudo-bags of X_i , where τ denotes the index of pseudo-bag.

2) *Multiple instance learning*: In the absence of instance-level labels, most MIL framework usually takes WSI bags as input and leverages a neural network to learn bag-level representations by aggregating multiple instance embeddings, followed by an MLP (multi-layer perceptron) to output slide-level predictions, $\hat{y}_1, \dots, \hat{y}_N$, as illustrated in Figure 3(a). This framework is also called embedding-level MIL [18].

B. Pseudo-bag Mixup augmentation

As shown in Figure 3(b), our scheme has three necessary steps: i) phenotype and pseudo-bag dividing, ii) bag-level mixing, and iii) target-level mixing. Next, we will describe their implementation details one by one.

1) *Phenotype and pseudo-bag division*: To align bag inputs in size for mixing, we cluster the instances of each bag into l different phenotypes, and then adopt phenotype-stratified sampling to obtain n instance-disjoint pseudo-bags. Pseudo-bag division consists of three major sub-steps; their details are provided in Algorithm 1. (1) *Prototype-based clustering*. We roughly follow a bag-prototype-based clustering method [42] to calculate l initial instance clusters. Each cluster could be interpreted as a specific instance phenotype. We choose this bag-prototype-based method, rather than K-means, for computation efficiency. (2) *Phenotype fine-tuning*. As shown in Figure 3(b), we further improve cluster quality by fine-tuning phenotypes for k times, because initial clusters could not be desirable due to the possible biases in bag prototype estimation [42]. (3) *Phenotype-stratified sampling*. We randomly sample instances without replacement from each phenotype stratum, obtaining n pseudo-bags (each with roughly the same

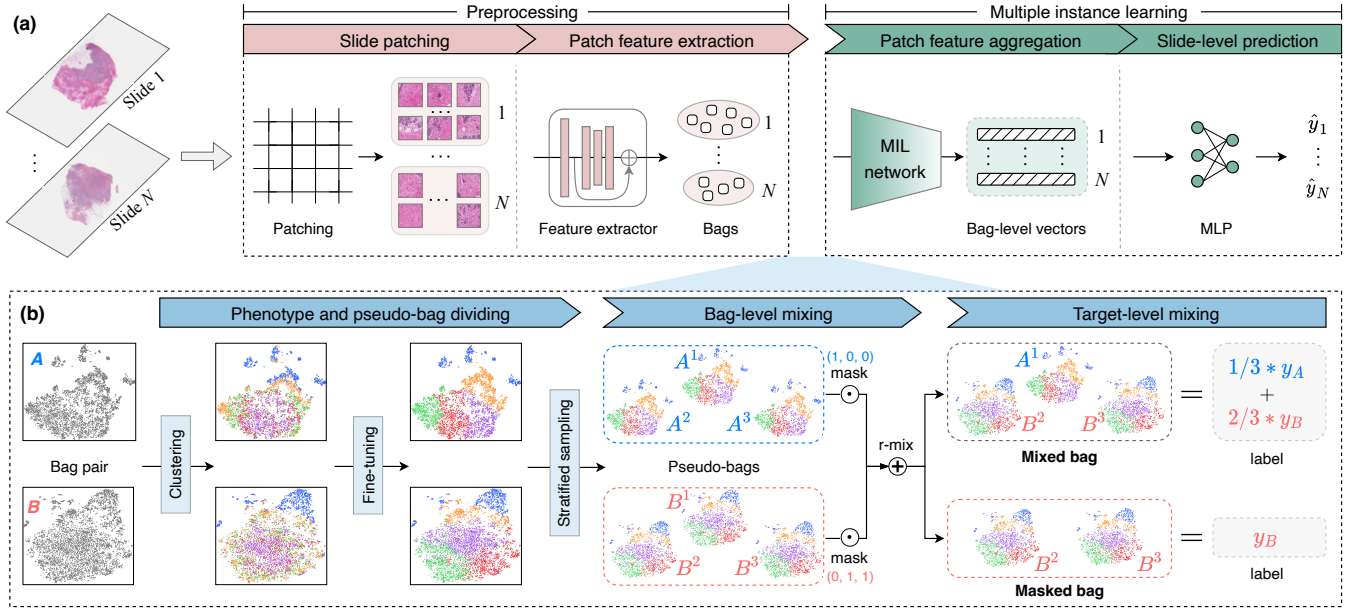


Fig. 3. PseMix data augmentation for MIL-based WSI classification. (a) Classical MIL paradigm for weakly-supervised WSI analysis. (b) Illustration of PseMix. Two WSI bags A and B are taken as examples. Solid rectangular boxes give the t-SNE visualization of instances, where scatter points represents instances and each color indicates a specific phenotype. A^1, A^2, \dots, B^3 are pseudo-bag notations. R-mix means random mixing.

instance numbers) from each bag. As a result, the time and space complexity of Algorithm 1 are $\mathcal{O}(lkm_i)$ and $\mathcal{O}(m_i)$, respectively. Given that l and k are usually set in $[10^0, 10^1]$, the procedure of pseudo-bag division can be executed in a linear time and space complexity *w.r.t.* instance number for each bag. Its actual computational cost is measured through experiments and presented in Section IV-E.

Previous studies of pseudo-bags [6], [11], [42] assume that *pseudo-bags could inherit labels from their parent bag*. This paper also follows this basic assumption. However, the inconsistent distribution between pseudo-bags and their parent bag may incur noises to pseudo-bag labels. Accordingly, in pseudo-bag dividing, we especially fine-tune phenotype clusters and adopt the way of phenotype-stratified sampling, to i) preserve the original phenotype distribution as much as possible in those divided pseudo-bags and ii) make pseudo-bags consistent with their parent bag in semantics. We will further evaluate and discuss different pseudo-bag division methods through comparative experiments.

2) *Bag-level mixing*: As illustrated in Figure 3(b), we augment WSI bags in this step by masking and random mixing (r-mix) on two input bags. Without loss of generality, let (A, B) denote any bag pair from original training samples, where $A, B \in \{1, 2, \dots, N\}$ and $A \neq B$. We further denote their respective pseudo-bags by $\{X_A^\tau\}_{\tau=1}^n$ and $\{X_B^\tau\}_{\tau=1}^n$, where pseudo-bags could be arranged in arbitrary orders.

(1) *Masking*. We randomly mask $1 - \lambda$ and λ pseudo-bags in A and B , respectively. Similar to Mixup [26], $\lambda \in [0, 1]$ is drawn from a Beta distribution, *i.e.*, $\lambda \sim \text{Beta}(\alpha, \alpha)$, where α is non-negative. We write two masked bags as follows:

$$X'_A = (1 - \mathbf{M}_\lambda) \odot \{X_A^\tau\}_{\tau=1}^n, \quad X'_B = \mathbf{M}_\lambda \odot \{X_B^\tau\}_{\tau=1}^n, \quad (3)$$

where $\mathbf{M}_\lambda \in \{0, 1\}^n$ is a binary mask indicating which pseudo-bag to mask and keep, $\sum \mathbf{M}_\lambda = \lfloor \lambda(n + 1) \rfloor$, and

Algorithm 1: Pseudo-bag division (for single bag).

Input: a WSI bag $X_i = \{x_{i,j}\}_{j=1}^{m_i}$, pseudo-bag number n , phenotype number l , fine-tuning times k .

Output: pseudo-bags $\{X_i^\tau\}_{\tau=1}^n$.

// Prototype-based clustering

```

1  $p_i \leftarrow \frac{1}{m_i} \sum_j x_{i,j}$  // bag prototype
2 initialize phenotype indicator  $C_i = \{c_{i,j}\}_{j=1}^{m_i}$ 
3 for  $j \leftarrow 1$  to  $m_i$  do
4    $s_{i,j} \leftarrow \cos(p_i, x_{i,j})$  // cosine similarity
5   let  $c \in \{1, 2, \dots, l\}$ 
6    $c_{i,j} \leftarrow \text{find a } c \text{ s.t. } s_{i,j} \in [-1 + \frac{2(c-1)}{l}, -1 + \frac{2c}{l})$ 
7 end
// Phenotype fine-tuning
8 for  $t \leftarrow 1$  to  $k$  do
9   initialize phenotype centroids  $\{f_{i,c} \in \mathbb{R}^d\}_{c=1}^l$ 
10  for  $c \leftarrow 1$  to  $l$  do
11     $I_c \leftarrow \{j \mid c_{i,j} = c\}$ 
12     $f_{i,c} \leftarrow \frac{1}{|I_c|} \sum_{j \in I_c} x_{i,j}$ 
13  end
14  for  $j \leftarrow 1$  to  $m_i$  do
15     $c_{i,j} \leftarrow \arg \min_c \cos(f_{i,c}, x_{i,j})$ 
16  end
17 end

```

// Phenotype-stratified sampling

```

18 initialize  $n$  empty pseudo-bags  $\{X_i^\tau = \emptyset\}_{\tau=1}^n$ 
19 for  $c \leftarrow 1$  to  $l$  do
20    $I_c \leftarrow \{j \mid c_{i,j} = c\}$ 
21   randomly and uniformly split  $I_c$  into  $n$  parts
22   fetch the instances w.r.t. the  $n$  parts of  $I_c$ 
23   append the instances to  $X_i^1, \dots, X_i^n$ , respectively
24 end

```

⊙ represents element-wise product.

(2) *Random mixing*. As depicted in Figure 3(b), our r-mix operation could output two kinds of augmented bags, *i.e.*, mixed or masked bags. Specifically, in r-mix, we let the masked bag X'_B join with X'_A or not join but directly output. For the first case, the output is a mixed bag:

$$\tilde{X} = (1 - \mathbf{M}_\lambda) \odot \{X'_A\}_{\tau=1}^n + \mathbf{M}_\lambda \odot \{X'_B\}_{\tau=1}^n. \quad (4)$$

It also consists of n pseudo-bags. In Equation 4, both of A and B are cast as n pseudo-bags and pseudo-bags are the minimum unit in mixing. All of these are the necessary prerequisites for size alignment and subsequent complementary masking operations (*i.e.*, \mathbf{M}_λ and $1 - \mathbf{M}_\lambda$). For the second case of not joining, the output is a masked bag:

$$X' = \mathbf{M}_\lambda \odot \{X'_B\}_{\tau=1}^n. \quad (5)$$

It is utilized as the other kind of augmented bags for training.

(3) *Motivation behind random mixing*. We introduce a simple random mixing mechanism into standard Mixup for two purposes: **i)** enhancing the diversity of training samples and **ii)** making models efficiently learn from vicinity samples (mixed bags). Pseudo-bag-masked bags could be viewed as the intermediate samples between original training data and synthetic mixed data. They could smooth the transition from original distribution to vicinity distribution, thereby helping models to efficiently learn from synthetic vicinity samples. We will evaluate and discuss r-mix in ablation study.

From Equation 3, 4, and 5, we can see that our bag-level mixing is decoupled from the stage of MIL. Consequently, our scheme could serve as a plugin-and-play data augmentation method for MIL, different from the RankMix [34] that relies on MIL model predictions for bag alignment.

3) *Target-level mixing*: For the mixed bag \tilde{X} , we adopt the same λ as that used in Equation 4 for target mixing, *i.e.*,

$$\tilde{y} = \lambda y_A + (1 - \lambda) y_B. \quad (6)$$

Intuitively, there are λ and $1 - \lambda$ pseudo-bags from A and B , in \tilde{X} . Given the assumption that pseudo-bags share the same label as their parent bag, the interpolation scale of y_A and y_B could be set to λ (based on pseudo-bag mixing ratio) for semantic alignment. For the masked bag X' , we set $y' = y_B$, also following the basic assumption of pseudo-bags.

Let \mathcal{D}_{aug} denote the final training data augmented by our PseMix. It thus contains (\tilde{X}, \tilde{y}) and (X', y') . In our implementation, we adjust their proportion in \mathcal{D}_{aug} by adopting a hyper-parameter $p \in [0, 1]$ to set the probability of joining or mixing in r-mix. Therefore, \mathcal{D}_{aug} is written as follows:

$$\mathcal{D}_{\text{aug}} = \begin{cases} (\tilde{X}, \tilde{y}) & \text{with a probability of } p, \\ (X', y') & \text{with a probability of } 1 - p. \end{cases} \quad (7)$$

IV. EXPERIMENTS

In this section, we mainly evaluate the effectiveness and advantages of PseMix through comparative experiments and ablation studies. We describe experimental settings in Section IV-A. Then we validate PseMix using three different tasks and compare it with other related data augmentation methods in

Section IV-B. In Section IV-C and IV-D, we show the advantages of PseMix in generalization and robustness. Finally, ablation studies and hyper-parameter sensitivity analysis are presented in Section IV-E and IV-F, respectively.

A. Experimental settings

1) *Datasets and tasks*: We use the following pathology diagnosis tasks in this study: 1) invasive breast carcinoma (BRCA) subtyping for IDC (Invasive Ductal Carcinoma) and ILC (Invasive Lobular Carcinoma), 2) LUAD (Lung Adenocarcinoma) and LUSC (Lung Squamous Cell Carcinoma) recognition in Non-Small Cell Lung Carcinoma (NSCLC), and 3) Renal Cell Carcinoma (RCC) classification for Clear Cell, Papillary, and Chromophobe. These three tasks are often adopted to evaluate MIL models [9], [19]. Their respective datasets are publicly-available at TCGA (<https://portal.gdc.cancer.gov>). As shown in Table II, 2,740 slides are collected. They are preprocessed with the tools developed by CLAM [7].

TABLE II
STATISTICAL DETAILS OF THREE WSI DATASETS.

| Item | BRCA | NSCLC | RCC |
|---------------------|-----------|-----------|-----------|
| # Patients | 898 | 947 | 895 |
| # Slides | 953 | 1,044 | 937 |
| # Patches | 2,961,552 | 3,235,064 | 3,317,384 |
| # Patches per slide | 3,107.6 | 3098.7 | 3,540.4 |

2) *Performance evaluation*: We randomly split each dataset into training, validation, and test sets on the patient level, with a ratio of 65:10:25, where the validation set is used for early stopping and model selection. 4-fold cross-validation (cv) is adopted. The two classification metrics, Area Under the Curve (AUC) and accuracy (ACC), are used. And we report their mean and standard deviation across 4 folds. For ACC calculation, the class with the largest probability is taken as classification prediction. In addition, we assess the generalization ability of models by measuring the AUC and loss gap between training and test set, following [20], [21].

3) *Implementation details*: ABMIL [18], DSMIL [8], and TransMIL [9] are employed as MIL backbones for experiments, as they are frequently used in WSI classification. We follow their official codes for model implementation. A truncated ResNet-50 model [44] pre-trained on ImageNet [45] is utilized as the feature extractor and $d = 1024$, following [7]. α is set to 1 by default, which means that λ is distributed uniformly over $[0, 1]$. For the hyper-parameters of pseudo-bag division, we empirically set $n = 30$ and $l = k = 8$ by default across all used datasets and networks. We will analyze important hyper-parameters in Section IV-F. All experiments are run on a machine with two NVIDIA GeForce RTX 3090 GPUs. Please refer to our codes (<https://github.com/liupeii01/PseMix>) for more details.

B. Classification performance

We first verify whether PseMix could help improve the classification performance of MIL models. The models trained without any data augmentation, *i.e.*, vanilla models, are taken

TABLE III
CLASSIFICATION PERFORMANCE OF VANILLA MIL MODELS AND PSEMIX-BASED ONES ON THREE WSI DATASETS.

| Network | Method | BRCA | | NSCLC | | RCC | | Average (%) | |
|----------------|------------------|---------------------|---------------------|---------------------|---------------------|---------------------|---------------------|--------------|--------------|
| | | ACC (%) | AUC (%) | ACC (%) | AUC (%) | ACC (%) | AUC (%) | ACC | AUC |
| ABMIL [18] | vanilla | 86.34 ± 1.97 | 87.05 ± 2.97 | 83.88 ± 4.94 | 92.23 ± 2.81 | 88.90 ± 1.20 | 97.36 ± 1.10 | 86.37 | 92.21 |
| | w/ ReMix | 86.46 ± 1.67 | 87.74 ± 3.97 | 84.48 ± 3.99 | 91.66 ± 2.04 | 88.24 ± 1.99 | 96.93 ± 0.90 | 86.39 | 92.11 |
| | w/ Mixup | 85.91 ± 2.09 | 87.31 ± 3.54 | 86.02 ± 2.67 | 92.75 ± 2.47 | 90.39 ± 2.05 | 97.78 ± 0.76 | 87.44 | 92.61 |
| | w/ RankMix | 85.62 ± 1.34 | 87.48 ± 3.97 | 84.73 ± 1.70 | 91.76 ± 2.07 | 89.44 ± 2.00 | 97.37 ± 0.68 | 86.60 | 92.20 |
| | w/ InstanceMix | 86.24 ± 1.94 | 87.98 ± 3.18 | 84.83 ± 2.76 | 91.74 ± 2.22 | 88.73 ± 1.96 | 97.60 ± 0.41 | 86.60 | 92.44 |
| | w/ PseMix (ours) | 86.64 ± 3.11 | 89.49 ± 3.69 | 86.45 ± 3.28 | 93.01 ± 2.06 | 90.50 ± 1.66 | 98.02 ± 0.55 | 87.86 | 93.51 |
| Δ over vanilla | + 0.30 | + 2.44 | + 2.57 | + 0.78 | + 1.60 | + 0.66 | + 1.49 | + 1.30 | |
| DSMIL [8] | vanilla | 86.75 ± 1.48 | 87.73 ± 2.04 | 85.70 ± 3.18 | 92.99 ± 2.94 | 89.81 ± 3.29 | 97.65 ± 0.81 | 87.42 | 92.79 |
| | w/ ReMix | 85.74 ± 2.38 | 87.98 ± 3.59 | 83.30 ± 3.71 | 91.59 ± 2.06 | 87.49 ± 1.30 | 96.54 ± 1.74 | 85.51 | 92.04 |
| | w/ Mixup | 86.35 ± 2.26 | 88.30 ± 3.10 | 87.52 ± 3.12 | 94.22 ± 2.39 | 90.60 ± 2.29 | 97.77 ± 0.85 | 88.16 | 93.43 |
| | w/ RankMix | 84.80 ± 1.73 | 86.49 ± 2.58 | 86.39 ± 3.33 | 93.51 ± 2.69 | 90.27 ± 1.25 | 97.38 ± 0.87 | 87.15 | 92.46 |
| | w/ InstanceMix | 85.39 ± 3.23 | 87.94 ± 3.48 | 86.45 ± 3.39 | 92.40 ± 2.09 | 89.48 ± 2.28 | 97.54 ± 0.55 | 87.11 | 92.63 |
| | w/ PseMix (ours) | 88.22 ± 2.65 | 89.65 ± 3.19 | 88.68 ± 2.19 | 93.92 ± 2.19 | 90.62 ± 1.20 | 97.89 ± 0.44 | 89.17 | 93.82 |
| Δ over vanilla | + 1.47 | + 1.92 | + 2.98 | + 0.93 | + 0.81 | + 0.24 | + 1.75 | + 1.03 | |
| TransMIL [9] | vanilla | 85.31 ± 0.65 | 88.83 ± 1.37 | 85.31 ± 4.01 | 92.14 ± 2.56 | 90.61 ± 1.62 | 97.88 ± 0.80 | 87.08 | 92.95 |
| | w/ ReMix | 79.88 ± 2.12 | 78.76 ± 4.17 | 83.27 ± 3.05 | 90.67 ± 3.02 | 87.52 ± 2.53 | 96.60 ± 1.04 | 83.56 | 88.68 |
| | w/ Mixup | 81.52 ± 2.39 | 88.41 ± 3.07 | 87.62 ± 3.76 | 94.52 ± 2.49 | 91.03 ± 1.60 | 97.88 ± 0.64 | 86.72 | 93.60 |
| | w/ RankMix | 84.69 ± 1.13 | 87.73 ± 1.31 | 86.45 ± 2.66 | 93.75 ± 2.54 | 90.63 ± 1.92 | 97.97 ± 0.51 | 87.26 | 93.15 |
| | w/ InstanceMix | 86.77 ± 2.35 | 89.44 ± 3.01 | 86.74 ± 2.25 | 92.72 ± 2.34 | 91.04 ± 1.57 | 97.84 ± 0.31 | 88.18 | 93.33 |
| | w/ PseMix (ours) | 86.98 ± 1.47 | 90.40 ± 2.29 | 87.67 ± 2.80 | 93.47 ± 1.91 | 91.14 ± 1.94 | 97.76 ± 0.69 | 88.60 | 93.88 |
| Δ over vanilla | + 1.67 | + 1.57 | + 2.36 | + 1.33 | + 0.53 | - 0.12 | + 1.52 | + 0.93 | |

as the baseline for comparison. Moreover, we run other input mixing methods (see Table I) for further comparisons. They are i) *ReMix* [33], which only mixes bags within the same class; ii) *Mixup* [26], the original interpolation-based Mixup in which two bags are aligned in instance number by random dropping; iii) *RankMix* [34], an improved interpolation-based one in which two bags are aligned firstly by instance ranking and then by instance dropping; iv) *InstanceMix*, an instance-level Mixup baseline in which two bags are mixed after masking some instances, rather than pseudo-bags, specially designed for the comparison to our pseudo-bag-level scheme. Besides data augmentation, other regular training settings are shared between all baselines and networks.

There are two apparent results in Table III. (1) PseMix almost always helps improve the performance of MIL models in WSI classification. Its average improvements over vanilla models are consistently positive across three MIL networks, ranging from 0.93% to 1.75%. (2) PseMix could often surpass other related input mixing methods in average ACC and AUC. Moreover, the maximum gap in average ACC between PseMix and others is 1.01% (when it is on DSMIL); as in average AUC, the maximum is 0.90% (when it is on ABMIL). These results suggest that our pseudo-bag Mixup scheme is an effective and superior Mixup variant for improving the performance of MIL models in WSI classification.

As described in Section III, our PseMix is a masking-based mixing, pseudo-bag-level Mixup scheme. It outperforms two interpolation-based variants and a masking-based instance-level variant in most cases. Moreover, it is superior to them in average metrics for three MIL networks. (1) For two interpolation-based variants, i.e., original Mixup and its improved RankMix, both of them often need to drop instances from the bag with more instances, to align two irregular bags for interpolation. This operation may result in artificial

information loss, especially when there is a big gap in instance numbers. Furthermore, interpolation-based Mixup often performs worse than masking-based ones in image classification, since interpolation operations equally treat the background and foreground in images, as demonstrated in [29]. By contrast, our PseMix does not rely on interpolation but masks pseudo-bags for bag mixing. (2) For InstanceMix, it is based on masking like PseMix but operates at the instance level. And it treats all instances equally, without the critical semantic alignment for Mixup. Our PseMix tackles this by manipulating pseudo-bags. For those reasons, PseMix could often perform better than previous Mixup variants in WSI classification.

C. Generalization test

Most previous works of WSI classification usually focus on promoting classification performance, rarely concerned with model generalization. Here we demonstrate another benefit of PseMix, i.e., better model generalization.

1) *Generalization gap*: Following [20], [21], we measure the generalization gap between training and test sets to assess model generalization. We have the following observations from Figure 4. (1) Vanilla models always perform better on training set but worse on test set in training. (2) By contrast, their PseMix-based counterparts often have lower test losses and higher test AUCs, showing smaller generalization gaps. An intuitive, possible explanation is that PseMix enables MIL models to learn from the new training samples drawn from vicinity distribution and likely expand their generalization boundary, thus performing better on test data.

2) *Test on in-between training data*: We further examine the model performance on out-of-distribution data. Specifically, we synthesize new in-between data for testing by applying Equation 4 to training samples. From the test results shown in Figure 5, we could see that i) the cross-entropy loss

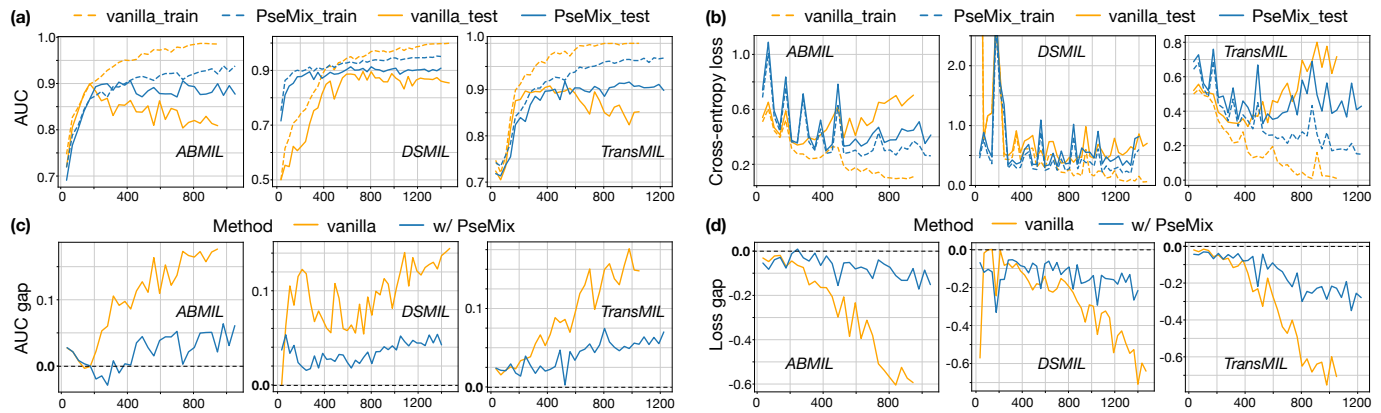


Fig. 4. Generalization gap (AUC and cross-entropy loss) between training and test set. Three MIL networks are trained on BRCA.

TABLE IV
ROBUSTNESS AGAINST PATCH OCCLUSION.

| Patch masking | Method | ABMIL | | DSMIL | | TransMIL | | Average (%) | |
|---------------|-----------|---------------------|---------------------|---------------------|---------------------|---------------------|---------------------|--------------|--------------|
| | | ACC (%) | AUC (%) | ACC (%) | AUC (%) | ACC (%) | AUC (%) | ACC | AUC |
| 20% | vanilla | 85.60 ± 2.14 | 87.13 ± 2.65 | 85.11 ± 1.87 | 86.94 ± 2.99 | 81.93 ± 2.44 | 87.51 ± 1.49 | 84.21 | 87.19 |
| | w/ PseMix | 87.27 ± 3.01 | 89.91 ± 3.05 | 86.96 ± 2.32 | 89.12 ± 3.90 | 87.07 ± 1.78 | 90.25 ± 2.53 | 87.10 | 89.76 |
| 40% | vanilla | 84.65 ± 3.02 | 86.86 ± 2.56 | 85.95 ± 2.03 | 87.07 ± 3.41 | 80.57 ± 4.20 | 86.28 ± 1.98 | 83.72 | 86.74 |
| | w/ PseMix | 86.65 ± 2.63 | 89.87 ± 2.99 | 85.50 ± 2.77 | 88.77 ± 3.94 | 84.77 ± 3.63 | 89.61 ± 2.02 | 85.64 | 89.42 |
| 60% | vanilla | 85.17 ± 3.44 | 87.05 ± 2.57 | 84.57 ± 2.25 | 86.94 ± 3.65 | 76.43 ± 10.16 | 84.26 ± 2.85 | 82.06 | 86.08 |
| | w/ PseMix | 86.65 ± 2.63 | 89.64 ± 3.04 | 84.77 ± 2.58 | 88.85 ± 4.07 | 82.27 ± 6.11 | 88.02 ± 2.27 | 84.56 | 88.84 |
| 80% | vanilla | 84.44 ± 2.85 | 87.05 ± 1.88 | 84.26 ± 2.51 | 86.43 ± 3.27 | 64.44 ± 19.91 | 76.82 ± 4.90 | 77.71 | 83.43 |
| | w/ PseMix | 85.06 ± 5.09 | 88.88 ± 3.43 | 80.71 ± 4.31 | 87.28 ± 4.71 | 78.92 ± 5.80 | 84.43 ± 6.18 | 81.56 | 86.86 |

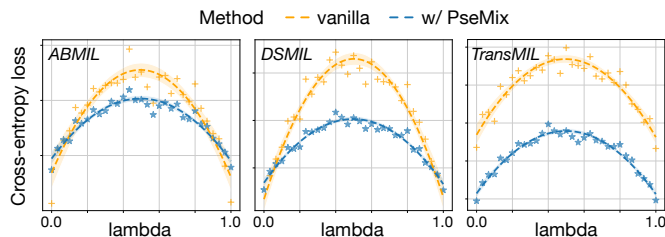


Fig. 5. Cross-entropy loss of in-between training data and their corresponding soft-labels.

on mixed data would become higher when the mix ratio λ approaches 0.5, *i.e.*, when making mixed bags far from both of two input bags; ii) it is clear that the models trained with PseMix often show lower test losses on out-of-distribution data points (*i.e.*, $0.0 < \lambda < 1.0$). The second observation is consistent with our intuitive explanation to PseMix, *i.e.*, PseMix-based models often perform better on mixed in-between data, suggesting that they indeed have learned from vicinity samples.

D. Robustness test

Here we further demonstrate yet another benefit of our PseMix data augmentation scheme, *i.e.*, improved models robustness. BRCA is used in this test.

1) *Robustness against patch occlusion:* We randomly mask the instances of bags of test set samples and then use them for

testing. From Table IV, we observe that PseMix-based models almost always obtain clear improvements over vanilla ones in various masking ratios. These improvements range from 1.92% to 3.85% and 2.57% to 3.43% in average ACC and AUC, apparently larger than those gains shown in Table III. These facts suggest that our PseMix also could help models in the robustness to patch occlusion.

2) *Robustness against label corruption:* To evaluate the model’s robustness to noisy labels, we use label-corrupted training samples to train MIL models. Specifically, some training samples are randomly selected and then tagged with any one random class label, following [26]. Results are reported on original test sets using the best (at the epoch with minimum validation loss) and the last models (at the last epoch).

As shown in Table V, (1) we find that the models trained with our PseMix often show great performance gains, 7 out of 9 cases for the best epoch and 8 out of 9 cases for the last one. Moreover, in average performance, PseMix-based models consistently exceed vanilla ones by large margins (1.80% ~ 5.58% in AUC and 1.09% ~ 9.96% in ACC). Furthermore, (2) we notice that vanilla models often suffer from greater performance drops than PseMix-based ones, when changing the epoch from best to last. For instance, a vanilla ABMIL model drops by 6.94% in accuracy when turning to use the last model, for a 20% corruption ratio; whereas its PseMix-based counterpart only drops by 3.34% in the same case. These observations tell us that our PseMix could often help MIL models obtain better robustness to noisy labels in training.

TABLE V
ROBUSTNESS AGAINST LABEL CORRUPTION.

| Checkpoint | Label corruption | Method | ABMIL | | DSMIL | | TransMIL | | Average (%) | |
|------------|------------------|--------------|---------------------|----------------------|---------------------|---------------------|---------------------|---------------------|--------------|--------------|
| | | | ACC (%) | AUC (%) | ACC (%) | AUC (%) | ACC (%) | AUC (%) | ACC | AUC |
| Best epoch | 20% | vanilla | 84.55 ± 2.84 | 83.81 ± 4.83 | 83.51 ± 2.00 | 83.84 ± 4.20 | 81.96 ± 1.16 | 82.32 ± 2.74 | 83.34 | 83.32 |
| | | w/ PseMix | 84.54 ± 3.25 | 83.67 ± 4.66 | 85.80 ± 3.55 | 85.27 ± 4.93 | 84.87 ± 1.91 | 86.41 ± 3.98 | 85.07 | 85.12 |
| | 50% | vanilla | 80.82 ± 1.77 | 76.77 ± 4.15 | 79.96 ± 1.57 | 75.71 ± 3.95 | 79.85 ± 0.15 | 74.54 ± 5.60 | 80.21 | 75.67 |
| Last epoch | 20% | w/ PseMix | 81.35 ± 2.75 | 78.72 ± 2.33 | 83.62 ± 1.96 | 79.94 ± 4.89 | 81.95 ± 0.46 | 81.61 ± 2.75 | 82.31 | 80.09 |
| | | vanilla | 78.28 ± 0.99 | 62.81 ± 7.83 | 79.02 ± 1.10 | 59.40 ± 2.86 | 74.99 ± 3.98 | 53.92 ± 4.25 | 77.43 | 58.71 |
| | 80% | w/ PseMix | 78.28 ± 0.83 | 61.13 ± 8.78 | 79.75 ± 1.19 | 64.81 ± 2.77 | 77.53 ± 2.89 | 59.76 ± 6.02 | 78.52 | 61.90 |
| Last epoch | 20% | vanilla | 77.61 ± 4.23 | 77.07 ± 5.42 | 82.05 ± 1.17 | 80.91 ± 4.12 | 76.58 ± 2.20 | 77.31 ± 2.68 | 78.75 | 78.43 |
| | | w/ PseMix | 81.20 ± 2.29 | 80.53 ± 7.14 | 83.74 ± 4.66 | 82.71 ± 7.41 | 82.05 ± 1.31 | 82.52 ± 5.29 | 82.33 | 81.92 |
| | 50% | vanilla | 75.34 ± 3.05 | 70.01 ± 5.81 | 75.43 ± 3.48 | 73.04 ± 4.11 | 70.35 ± 3.77 | 68.94 ± 3.37 | 73.71 | 70.66 |
| Last epoch | 50% | w/ PseMix | 79.05 ± 5.08 | 75.14 ± 4.12 | 82.78 ± 0.90 | 78.08 ± 4.07 | 78.82 ± 2.11 | 75.51 ± 3.72 | 80.22 | 76.24 |
| | | 80% | vanilla | 58.03 ± 10.23 | 60.34 ± 5.37 | 55.75 ± 14.53 | 58.63 ± 9.27 | 53.67 ± 7.72 | 51.20 ± 3.45 | 55.82 |
| | w/ PseMix | 57.53 ± 9.73 | 60.16 ± 7.76 | 65.99 ± 11.58 | 63.82 ± 3.65 | 73.81 ± 6.00 | 57.82 ± 9.21 | 65.78 | 60.60 | |

TABLE VI
DIFFERENT METHODS OF PSEUDO-BAG DIVISION. FT INDICATES FINE-TUNING. \bar{T} IS THE AVERAGE TIME COST PER SLIDE FOR DIVISION.

| Network | Division method | BRCA | | NSCLC | | RCC | | Average (%) | | \bar{T} ($\times 10^{-2}s$) |
|----------|-----------------|--------------|--------------|--------------|--------------|--------------|--------------|--------------|--------------|------------------------------------|
| | | ACC (%) | AUC (%) | ACC (%) | AUC (%) | ACC (%) | AUC (%) | ACC | AUC | |
| ABMIL | random | 88.01 ± 2.53 | 89.30 ± 3.26 | 86.06 ± 2.71 | 91.77 ± 2.16 | 89.55 ± 1.82 | 97.68 ± 0.46 | 87.87 | 92.92 | 0.016 |
| | K-means | 86.97 ± 1.82 | 88.47 ± 2.35 | 85.21 ± 2.49 | 91.87 ± 1.92 | 89.95 ± 1.77 | 97.77 ± 0.46 | 87.38 | 92.70 | 154.329 |
| | prototype | 86.33 ± 3.30 | 89.18 ± 3.36 | 86.06 ± 2.35 | 91.86 ± 2.20 | 89.66 ± 2.32 | 97.74 ± 0.46 | 87.35 | 92.93 | 0.129 |
| | prototype + FT | 87.50 ± 2.37 | 89.00 ± 3.74 | 86.32 ± 2.76 | 91.81 ± 2.40 | 90.08 ± 2.11 | 97.73 ± 0.47 | 87.97 | 92.85 | 0.382 |
| DSMIL | random | 86.45 ± 1.76 | 89.33 ± 3.50 | 85.80 ± 3.19 | 93.12 ± 1.93 | 88.93 ± 1.26 | 97.60 ± 0.37 | 87.06 | 93.35 | 0.016 |
| | K-means | 84.45 ± 2.97 | 87.53 ± 4.11 | 86.85 ± 2.31 | 92.91 ± 1.26 | 88.92 ± 1.26 | 97.50 ± 0.54 | 86.74 | 92.65 | 154.329 |
| | prototype | 86.25 ± 2.33 | 89.57 ± 3.50 | 86.06 ± 3.79 | 92.65 ± 1.95 | 88.62 ± 2.18 | 97.41 ± 0.61 | 86.98 | 93.21 | 0.129 |
| | prototype + FT | 87.28 ± 1.83 | 89.72 ± 3.65 | 85.91 ± 2.77 | 92.89 ± 1.60 | 89.56 ± 2.38 | 97.64 ± 0.54 | 87.58 | 93.42 | 0.382 |
| TransMIL | random | 86.67 ± 1.93 | 88.40 ± 2.37 | 84.31 ± 2.53 | 91.90 ± 1.74 | 90.53 ± 1.97 | 97.82 ± 0.19 | 87.17 | 92.71 | 0.016 |
| | K-means | 87.31 ± 1.80 | 89.18 ± 2.48 | 85.71 ± 2.41 | 92.65 ± 2.24 | 89.89 ± 1.89 | 97.78 ± 0.33 | 87.64 | 93.20 | 154.329 |
| | prototype | 86.24 ± 2.32 | 88.78 ± 2.02 | 85.72 ± 1.54 | 92.09 ± 0.80 | 89.86 ± 2.81 | 97.75 ± 0.27 | 87.27 | 92.87 | 0.129 |
| | prototype + FT | 86.65 ± 2.26 | 88.50 ± 3.52 | 86.22 ± 1.47 | 92.63 ± 1.63 | 90.83 ± 1.08 | 97.78 ± 0.23 | 87.90 | 92.97 | 0.382 |

E. Ablation study

1) *Study on different pseudo-bag division methods:* As described in Section III-B, different methods could be adopted to generate pseudo-bags, such as random sampling and phenotype-stratified sampling. Here we compare our adopted method, *i.e.*, bag-prototype-based clustering + phenotype fine-tuning (prototype + *ft*), with the other three, random sampling, K-means and bag-prototype-based stratified sampling. We set $p = 1$ for this study. Test results are presented in Table VI.

These test results indicate that our prototype + *ft* is competitive among four pseudo-bag division methods. Our evidences have three-fold. (1) prototype + *ft* could often obtain better overall performances than the other three, especially in average ACC. (2) It takes three orders of magnitude less time than the K-means-based one that also utilizes stratified sampling. (3) Compared to random and bag-prototype-based division, it merely introduces moderate time costs for phenotype clustering or fine-tuning but performs better in most cases.

2) *Study on random mixing:* Apart from pseudo-bag division, random mixing (r-mix) is also an critical design in PseMix. It could produce two kinds of augmented bags for training, mixing bags and masked bags. Here we conduct ablation studies on them and show the results in Table VII. From these results, we find that adopting both mixed and

masked bags for training could often obtain better average metrics (5 out of 6 cases), compared to only using mixed or masked bags. Data diversity may be one of the most straightforward explanations. Besides, it may be the involvement of masked bags that makes models learn from mixed bags (vicinity samples) more efficiently and thus obtain better performances. Because pseudo-bag-masked bags could be cast as the intermediate samples between original training data and synthetic mixed data, smoothing the transition from original distribution to vicinity distribution and thereby facilitating the efficient learning of models on vicinity samples.

F. Further analysis

Here we examine more experimental settings to understand their sensitivity to model performance. We mainly present the experimental results measured on BRCA.

1) *Other feature extractors:* Apart from the classical ResNet-50 model adopted in [7], we also try two more advanced feature extractors. They are HIPT [19] and CTransPath [46], pre-trained with self-supervised learning on WSIs. We directly use their released model weights for feature extraction. The test results of Table VIII reveal that PseMix still consistently improves the performance of vanilla models across three

TABLE VII

ABLATION STUDY. R-MIX MEANS RANDOM MIXING. MIX AND MASK INDICATES USING MIXED AND MASKED BAGS FOR TRAINING, RESPECTIVELY.

| Network | R-mix | | BRCA | | NSCLC | | RCC | | Average (%) | |
|----------|-------|------|---------------------|---------------------|---------------------|---------------------|---------------------|---------------------|--------------|--------------|
| | Mix | Mask | ACC (%) | AUC (%) | ACC (%) | AUC (%) | ACC (%) | AUC (%) | ACC | AUC |
| ABMIL | | ✓ | 85.71 ± 2.25 | 87.39 ± 2.38 | 85.11 ± 2.60 | 92.19 ± 1.87 | 90.38 ± 0.84 | 97.94 ± 0.74 | 87.07 | 92.51 |
| | ✓ | | 87.50 ± 2.37 | 89.00 ± 3.74 | 86.32 ± 2.76 | 91.81 ± 2.40 | 90.08 ± 2.11 | 97.73 ± 0.47 | 87.97 | 92.85 |
| | ✓ | ✓ | 86.64 ± 3.11 | 89.49 ± 3.69 | 86.45 ± 3.28 | 93.01 ± 2.06 | 90.50 ± 1.66 | 98.02 ± 0.55 | 87.86 | 93.51 |
| DSMIL | | ✓ | 85.72 ± 1.63 | 89.31 ± 2.83 | 86.96 ± 2.91 | 93.57 ± 2.49 | 90.50 ± 1.79 | 97.93 ± 0.48 | 87.73 | 93.60 |
| | ✓ | | 87.28 ± 1.83 | 89.72 ± 3.64 | 85.91 ± 2.77 | 92.89 ± 1.60 | 89.56 ± 2.38 | 97.64 ± 0.54 | 87.58 | 93.42 |
| | ✓ | ✓ | 88.22 ± 2.65 | 89.65 ± 3.19 | 88.68 ± 2.19 | 93.92 ± 2.19 | 90.62 ± 1.20 | 97.89 ± 0.44 | 89.17 | 93.82 |
| TransMIL | | ✓ | 86.56 ± 0.91 | 89.31 ± 1.22 | 87.13 ± 3.37 | 93.33 ± 1.61 | 90.16 ± 1.82 | 97.69 ± 0.94 | 87.95 | 93.44 |
| | ✓ | | 86.65 ± 2.26 | 88.50 ± 3.52 | 86.22 ± 1.47 | 92.63 ± 1.63 | 90.83 ± 1.08 | 97.78 ± 0.23 | 87.90 | 92.97 |
| | ✓ | ✓ | 86.98 ± 1.47 | 90.40 ± 2.29 | 87.67 ± 2.80 | 93.47 ± 1.91 | 91.14 ± 1.94 | 97.76 ± 0.69 | 88.60 | 93.88 |

TABLE VIII

DIFFERENT PATCH FEATURE EXTRACTORS.

| SSL-based feature extractor | Method | ABMIL | | DSMIL | | TransMIL | | Average (%) | |
|-----------------------------|-----------|---------------------|---------------------|---------------------|---------------------|---------------------|---------------------|--------------|--------------|
| | | ACC (%) | AUC (%) | ACC (%) | AUC (%) | ACC (%) | AUC (%) | ACC | AUC |
| HIPT | vanilla | 84.89 ± 2.44 | 86.21 ± 2.22 | 82.50 ± 2.04 | 83.31 ± 2.88 | 82.80 ± 2.48 | 83.88 ± 3.55 | 83.40 | 84.47 |
| | w/ PseMix | 85.09 ± 2.39 | 86.39 ± 2.85 | 85.50 ± 2.82 | 87.00 ± 2.92 | 84.89 ± 2.06 | 84.94 ± 3.44 | 85.16 | 86.11 |
| CTransPath | vanilla | 90.02 ± 1.99 | 92.83 ± 1.75 | 88.77 ± 1.74 | 92.58 ± 1.59 | 90.44 ± 1.46 | 92.97 ± 1.42 | 89.74 | 92.79 |
| | w/ PseMix | 90.85 ± 1.56 | 93.66 ± 2.11 | 89.28 ± 1.44 | 92.62 ± 2.18 | 91.38 ± 1.59 | 93.54 ± 2.02 | 90.50 | 93.27 |

MIL networks, even for different feature extractors. This result suggests the adaptability of PseMix.

2) *Hyper-parameter analysis*: We test the two most important hyper-parameters in PseMix, n (pseudo-bag number) and p (the probability of random mixing). Test results are shown in Figure 6. For n , a value near our default setting ($n = 30$) tends to obtain better metrics. All the hyper-parameters of pseudo-bag division are set by default across all datasets and networks without tuning. For p , a larger value is likely to result in better test performances. We set p to 0.8, 0.9, and 0.4 for ABMIL, DSMIL, and TransMIL, respectively, based on their respective losses on validation sets; the other values of p could obtain better results on test sets.

V. CONCLUSION

This paper proposes a Pseudo-bag Mixup (PseMix) data augmentation scheme for MIL-based WSI classification. It utilizes pseudo-bag concepts to fulfill Mixup alignment, thereby generalizing the Mixup strategy originally for general images to special WSIs. This scheme is compatible with most prevalent MIL paradigms. Moreover, it is efficient and plugin-and-play, neither involving time-consuming operations nor relying on the prediction of MIL models. Comparative experiments and ablation studies confirm that PseMix is an effective Mixup variant for WSI classification. It could often improve the performance of MIL models and obtain better overall performance than other related data mixing strategies. Other than that, it is observed that MIL models could often benefit more from PseMix in many other notable aspects, such as model generalization, patch occlusion robustness, and the robustness to noisy labels. In the future, our PseMix could serve as a promising data augmentation method to help develop the WSI classification models with better generalization and robustness for clinical pathology diagnosis.

REFERENCES

- [1] K. Bera, K. A. Schalper, D. L. Rimm, V. Velcheti, and A. Madabhushi, "Artificial intelligence in digital pathology — new tools for diagnosis and precision oncology," *Nature Reviews Clinical Oncology*, vol. 16, no. 11, pp. 703–715, 2019.
- [2] M. K. K. Niazi, A. V. Parwani, and M. N. Gurcan, "Digital pathology and artificial intelligence," *The Lancet Oncology*, vol. 20, no. 5, pp. e253–e261, 2019.
- [3] M. D. Zarella, D. Bowman, F. Aeffner, N. Farahani, A. Xthona, S. F. Absar, A. Parwani, M. Bui, and D. J. Hartman, "A Practical Guide to Whole Slide Imaging: A White Paper From the Digital Pathology Association," *Archives of Pathology & Laboratory Medicine*, vol. 143, no. 2, pp. 222–234, feb 2019.
- [4] C. Mercan, S. Aksoy, E. Mercan, L. G. Shapiro, D. L. Weaver, and J. G. Elmore, "Multi-instance multi-label learning for multi-class classification of whole slide breast histopathology images," *IEEE Transactions on Medical Imaging*, vol. 37, no. 1, pp. 316–325, 2018.

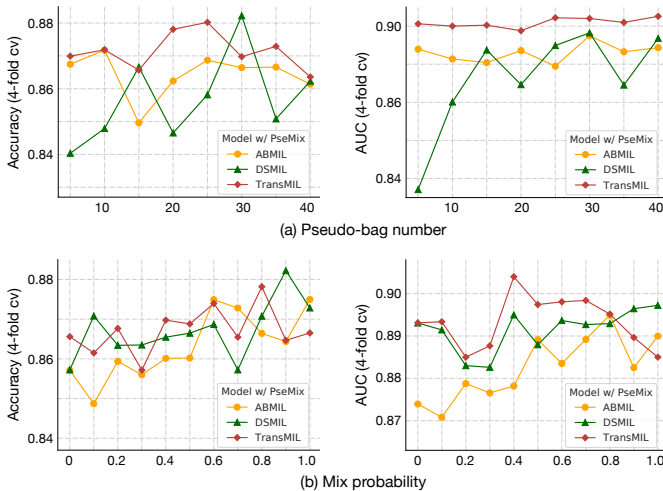


Fig. 6. Study on the two important hyper-parameters of PseMix, pseudo-bag number (n) and mix probability (p).

- [5] G. Campanella, M. G. Hanna, L. Geneslaw, A. Mirafior, V. Werneck Krauss Silva, K. J. Busam, E. Brogi, V. E. Reuter, D. S. Klimstra, and T. J. Fuchs, "Clinical-grade computational pathology using weakly supervised deep learning on whole slide images," *Nature Medicine*, vol. 25, no. 8, pp. 1301–1309, aug 2019.
- [6] W. Shao, T. Wang, Z. Huang, Z. Han, J. Zhang, and K. Huang, "Weakly supervised deep ordinal cox model for survival prediction from whole-slide pathological images," *IEEE Transactions on Medical Imaging*, vol. 40, no. 12, pp. 3739–3747, 2021.
- [7] M. Y. Lu, D. F. K. Williamson, T. Y. Chen, R. J. Chen, M. Barbieri, and F. Mahmood, "Data-efficient and weakly supervised computational pathology on whole-slide images," *Nature Biomedical Engineering*, vol. 5, no. 6, pp. 555–570, jun 2021.
- [8] B. Li, Y. Li, and K. W. Eliceiri, "Dual-stream multiple instance learning network for whole slide image classification with self-supervised contrastive learning," in *Proceedings of the IEEE/CVF Conference on Computer Vision and Pattern Recognition*, 2021, pp. 14 318–14 328.
- [9] Z. Shao, H. Bian, Y. Chen, Y. Wang, J. Zhang, X. Ji, and Y. Zhang, "TransMIL: Transformer based correlated multiple instance learning for whole slide image classification," in *Advances in Neural Information Processing Systems*, A. Beygelzimer, Y. Dauphin, P. Liang, and J. W. Vaughan, Eds., 2021.
- [10] Z. Wang, L. Yu, X. Ding, X. Liao, and L. Wang, "Lymph node metastasis prediction from whole slide images with transformer-guided multiinstance learning and knowledge transfer," *IEEE Transactions on Medical Imaging*, vol. 41, no. 10, pp. 2777–2787, 2022.
- [11] H. Zhang, Y. Meng, Y. Zhao, Y. Qiao, X. Yang, S. E. Coupland, and Y. Zheng, "Dtf-d-mil: Double-tier feature distillation multiple instance learning for histopathology whole slide image classification," in *Proceedings of the IEEE Conference on Computer Vision and Pattern Recognition*, 2022, pp. 18 802–18 812.
- [12] P. Liu, L. Ji, F. Ye, and B. Fu, "Advmil: Adversarial multiple instance learning for the survival analysis on whole-slide images," 2023.
- [13] Z. Zhu, L. Yu, W. Wu, R. Yu, D. Zhang, and L. Wang, "MuRCL: Multi-Instance Reinforcement Contrastive Learning for Whole Slide Image Classification," *IEEE Transactions on Medical Imaging*, vol. 42, no. 5, pp. 1337–1348, 2023.
- [14] Y. Zheng, J. Li, J. Shi, F. Xie, J. Huai, M. Cao, and Z. Jiang, "Kernel Attention Transformer for Histopathology Whole Slide Image Analysis and Assistant Cancer Diagnosis," *IEEE Transactions on Medical Imaging*, pp. 1–1, 2023.
- [15] J. Shi, L. Tang, Y. Li, X. Zhang, Z. Gao, Y. Zheng, C. Wang, T. Gong, and C. Li, "A structure-aware hierarchical graph-based multiple instance learning framework for pt staging in histopathological image," *IEEE Transactions on Medical Imaging*, pp. 1–1, 2023.
- [16] N. A. Koochbanani, B. Unnikrishnan, S. A. Khurram, P. Krishnaswamy, and N. Rajpoot, "Self-path: Self-supervision for classification of pathology images with limited annotations," *IEEE Transactions on Medical Imaging*, vol. 40, no. 10, pp. 2845–2856, 2021.
- [17] Z. Wang, C. Saoud, S. Wangsiricharoen, A. W. James, A. S. Popel, and J. Sulam, "Label cleaning multiple instance learning: Refining coarse annotations on single whole-slide images," *IEEE Transactions on Medical Imaging*, vol. 41, no. 12, pp. 3952–3968, 2022.
- [18] M. Ilse, J. Tomczak, and M. Welling, "Attention-based deep multiple instance learning," in *International conference on machine learning*, PMLR, 2018, pp. 2127–2136.
- [19] R. J. Chen, C. Chen, Y. Li, T. Y. Chen, A. D. Trister, R. G. Krishnan, and F. Mahmood, "Scaling Vision Transformers to Gigapixel Images via Hierarchical Self-Supervised Learning," in *2022 IEEE/CVF Conference on Computer Vision and Pattern Recognition (CVPR)*. IEEE, 2022, pp. 16 123–16 134.
- [20] Y. Jiang, D. Krishnan, H. Mobahi, and S. Bengio, "Predicting the generalization gap in deep networks with margin distributions," in *International Conference on Learning Representations*, 2019.
- [21] L. Zhang, Z. Deng, K. Kawaguchi, A. Ghorbani, and J. Zou, "How does mixup help with robustness and generalization?" in *International Conference on Learning Representations*, 2021.
- [22] V. N. Vapnik, *The Nature of Statistical Learning Theory*. New York, NY: Springer New York, nov 2000, vol. 41, no. 4.
- [23] C. Szegedy, W. Zaremba, I. Sutskever, J. Bruna, D. Erhan, I. Goodfellow, and R. Fergus, "Intriguing properties of neural networks," 2014.
- [24] C. Zhang, S. Bengio, M. Hardt, B. Recht, and O. Vinyals, "Understanding deep learning requires rethinking generalization," in *International Conference on Learning Representations*, 2017.
- [25] Z. Li, K. Kamnitsas, and B. Glocker, "Analyzing overfitting under class imbalance in neural networks for image segmentation," *IEEE Transactions on Medical Imaging*, vol. 40, no. 3, pp. 1065–1077, 2021.
- [26] H. Zhang, M. Cisse, Y. N. Dauphin, and D. Lopez-Paz, "mixup: Beyond empirical risk minimization," in *International Conference on Learning Representations*, 2018.
- [27] S. Yun, D. Han, S. Chun, S. J. Oh, Y. Yoo, and J. Choe, "Cutmix: Regularization strategy to train strong classifiers with localizable features," in *2019 IEEE/CVF International Conference on Computer Vision (ICCV)*, 2019, pp. 6022–6031.
- [28] J.-H. Kim, W. Choo, and H. O. Song, "Puzzle mix: Exploiting saliency and local statistics for optimal mixup," in *Proceedings of the 37th International Conference on Machine Learning*, ser. Proceedings of Machine Learning Research, vol. 119. PMLR, 2020, pp. 5275–5285.
- [29] J.-N. Chen, S. Sun, J. He, P. Torr, A. Yuille, and S. Bai, "Transmix: Attend to mix for vision transformers," in *2022 IEEE/CVF Conference on Computer Vision and Pattern Recognition (CVPR)*, 2022, pp. 12 125–12 134.
- [30] X. Han, Z. Jiang, N. Liu, and X. Hu, "G-mixup: Graph data augmentation for graph classification," in *Proceedings of the 39th International Conference on Machine Learning*, ser. Proceedings of Machine Learning Research, K. Chaudhuri, S. Jegelka, L. Song, C. Szepesvari, G. Niu, and S. Sabato, Eds., vol. 162. PMLR, 17–23 Jul 2022, pp. 8230–8248.
- [31] Y. Wang, J. Wang, J. Li, Z. Zhao, G. Chen, A. Liu, and P.-A. Heng, "Pointpatchmix: Point cloud mixing with patch scoring," 2023.
- [32] H. Gong, G. Chen, M. Mao, Z. Li, and G. Li, "Vqamix: Conditional triplet mixup for medical visual question answering," *IEEE Transactions on Medical Imaging*, vol. 41, no. 11, pp. 3332–3343, 2022.
- [33] J. Yang, H. Chen, Y. Zhao, F. Yang, Y. Zhang, L. He, and Y. Yao, "Remix: A general and efficient framework for multiple instance learning based whole slide image classification," in *Medical Image Computing and Computer Assisted Intervention*, 2022, p. 35–45.
- [34] Y.-C. Chen and C.-S. Lu, "Rankmix: Data augmentation for weakly supervised learning of classifying whole slide images with diverse sizes and imbalanced categories," in *Proceedings of the IEEE/CVF Conference on Computer Vision and Pattern Recognition (CVPR)*, June 2023, pp. 23 936–23 945.
- [35] I. Zaffar, G. Jaume, N. Rajpoot, and F. Mahmood, "Embedding space augmentation for weakly supervised learning in whole-slide images," 2022.
- [36] M. Kang, H. Song, S. Park, D. Yoo, and S. Pereira, "Benchmarking self-supervised learning on diverse pathology datasets," in *Proceedings of the IEEE/CVF Conference on Computer Vision and Pattern Recognition (CVPR)*, June 2023, pp. 3344–3354.
- [37] X. Guo, C. Yang, Y. Liu, and Y. Yuan, "Learn to threshold: Thresholdnet with confidence-guided manifold mixup for polyp segmentation," *IEEE Transactions on Medical Imaging*, vol. 40, no. 4, pp. 1134–1146, 2021.
- [38] C. Shorten and T. M. Khoshgoftaar, "A survey on image data augmentation for deep learning," *Journal of big data*, vol. 6, no. 1, pp. 1–48, 2019.
- [39] D. Tellez, G. Litjens, P. Bándi, W. Bulten, J.-M. Bokhorst, F. Ciompi, and J. van der Laak, "Quantifying the effects of data augmentation and stain color normalization in convolutional neural networks for computational pathology," *Medical Image Analysis*, vol. 58, p. 101544, 12 2019.
- [40] S. Cheng, S. Liu, J. Yu, G. Rao, Y. Xiao, W. Han, W. Zhu, X. Lv, N. Li, J. Cai, Z. Wang, X. Feng, F. Yang, X. Geng, J. Ma, X. Li, Z. Wei, X. Zhang, T. Quan, S. Zeng, L. Chen, J. Hu, and X. Liu, "Robust whole slide image analysis for cervical cancer screening using deep learning," *Nature Communications*, vol. 12, p. 5639, 9 2021.
- [41] Z. Shao, L. Dai, Y. Wang, H. Wang, and Y. Zhang, "Augdiff: Diffusion based feature augmentation for multiple instance learning in whole slide image," 2023.
- [42] R. Yang, P. Liu, and L. Ji, "Protodiv: Prototype-guided division of consistent pseudo-bags for whole-slide image classification," 2023.
- [43] Y. Cui, Z. Liu, X. Liu, X. Liu, C. Wang, T.-W. Kuo, C. J. Xue, and A. B. Chan, "Bayes-MIL: A new probabilistic perspective on attention-based multiple instance learning for whole slide images," in *The Eleventh International Conference on Learning Representations*, 2023.
- [44] K. He, X. Zhang, S. Ren, and J. Sun, "Deep Residual Learning for Image Recognition," in *2016 IEEE Conference on Computer Vision and Pattern Recognition (CVPR)*. IEEE, jun 2016, pp. 770–778.
- [45] J. Deng, W. Dong, R. Socher, L.-J. Li, Kai Li, and Li Fei-Fei, "ImageNet: A large-scale hierarchical image database," in *2009 IEEE Conference on Computer Vision and Pattern Recognition*. IEEE, jun 2009, pp. 248–255.
- [46] X. Wang, S. Yang, J. Zhang, M. Wang, J. Zhang, W. Yang, J. Huang, and X. Han, "Transformer-based unsupervised contrastive learning for histopathological image classification," *Medical Image Analysis*, vol. 81, p. 102559, 2022.